Article

# Spontaneous Compositional Nanopatterning in Li-Containing Perovskite Oxides

Beth S. Guiton, and Peter K. Davies

*J. Am. Chem. Soc.*, **2008**, 130 (50), 17168-17173 • DOI: 10.1021/ja806130u • Publication Date (Web): 17 November 2008



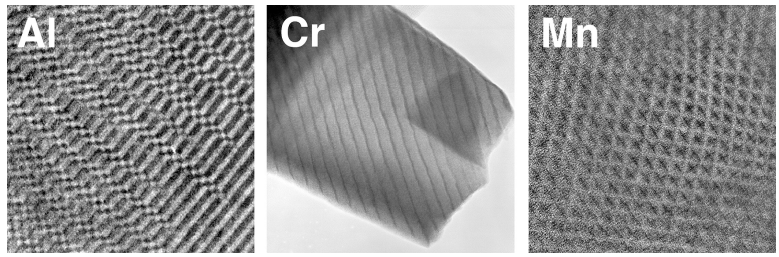


## More About This Article

Additional resources and features associated with this article are available within the HTML version:

- Supporting Information
- Access to high resolution figures
- Links to articles and content related to this article
- Copyright permission to reproduce figures and/or text from this article

View the Full Text HTML

J|A|C|S
ARTICLES

Published on Web 11/17/2008

# Spontaneous Compositional Nanopatterning in Li-Containing Perovskite Oxides

Beth S. Guiton and Peter K. Davies*

*Department of Materials Science and Engineering, University of Pennsylvania, 3231 Walnut Street, Philadelphia, Pennsylvania 19104*

Received August 5, 2008; E-mail: davies@seas.upenn.edu

***Abstract:*** A structure designed to show functionality on the nanometer length scale ideally would spontaneously form periodic nanometer-scale patterns comprising regions with contrasting properties. Here we report the synthesis of three new oxides that spontaneously form a variety of nanostructures with a periodic arrangement of phases with compositional and functional contrast. This is achieved through the partial substitution of Ti by Al, Cr, and Mn in periodically phase-separated $(Nd_{2/3-x}Li_{3x})TiO_3$ nanochessboard structures. The generality of this spontaneous compositional nanopatterning is promising for an array of exotic bulk and nanostructural properties.

## Introduction

The fabrication of nanostructures has been approached using several methods, such as "top-down" lithographic techniques and the "bottom-up" approach of wet chemistry. To exploit functionality on the nanometer length scale a structure ideally would spontaneously form patterns with uniform periodicity on a length scale designed to exploit nanoscale size effects, comprising regions with contrasting properties.[1] Solid-state self-assembly is an especially intriguing approach and has been used recently to form "nanochessboard"-type morphologies, for example, in a series of spinel solid solutions, which phase separate to form pseudoperiodic chessboard-like structures with promising potential magnetic functionalities.[2−4] More recently we reported[5] a perovskite solid solution with extremely uniform, tunable periodicities and phase-separated regions at the desired nanoscale yet little functional contrast between the two paramagnetic insulating phases. Here we report the synthesis of three new $Al^{3+}$-, $Cr^{3+}$-, and $Mn^{3+}$-containing perovskites that spontaneously form nanopatterned structures with a periodic arrangement of phases with compositional and functional contrast.

The nanochessboard superlattices occur in the solid solution of the Li-ion conducting perovskite $(Nd_{2/3-x}Li_{3x})TiO_3$ in which phase separation into a superlattice of nanodomains comprising $(Nd_{1/2}Li_{1/2})TiO_3$ separated by a zigzagging boundary region comprising $Nd_{2/3}TiO_3$ leads to extremely periodic diamond-like nanostructures (Figure 1).[5] The phase separation leads to a concurrent chessboard pattern in the strain field, which is imaged simultaneously at low resolution in the transmission electron microscope (TEM). The materials reported here have been doped

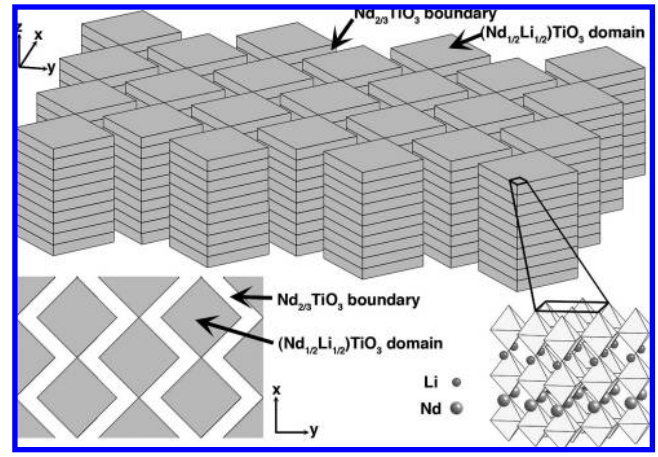


***Figure 1.*** Periodic phase separation in $(Nd_{2/3-x}Li_{3x})TiO_3$. (Top) Three-dimensional representation showing the stacking of square nanodomains along the *z* direction. (Bottom left) View along the *z* direction showing the diamond-like structure formed. This letter reports the attempt to replace the $Ti^{4+}$ cations in the boundary region with $Al^{3+}$, $Cr^{3+}$, and $Mn^{3+}$ to give boundary compositions of $NdAlO_3$, $NdCrO_3$, and $NdMnO_3$, respectively. (Bottom right) Polyhedral model showing $TiO_6$ octahedra and the (001) A-site layering of Nd and Li in the domain region.

so as to replace the $Ti^{4+}$ in the boundary $Nd_{2/3}TiO_3$ phase with $Al^{3+}$, $Cr^{3+}$, and $Mn^{3+}$ in an attempt to exchange this end member for $NdAlO_3$, $NdCrO_3$, and $NdMnO_3$, respectively. Although $Al^{3+}$, $Cr^{3+}$, and $Mn^{3+}$ doping has been studied extensively for the La- and Pr-based lithium titanate perovskites,[6−15] to the best

(1) *Nat. Mater.* **2007**, *6*, 87.
(2) Yeo, S.; Horibe, Y.; Mori, S.; Tseng, C. M.; Chen, C. H.; Khachaturyan, A. G.; Zhang, C. L.; Cheong, S.-W. *Appl. Phys. Lett.* **2006**, *89*, 233120.
(3) Zhang, C. L.; Tseng, C. M.; Chen, C. H.; Yeo, S.; Choi, Y. J.; Cheong, S.-W. *Appl. Phys. Lett.* **2007**, *91*, 233110.
(4) Zhang, C. L.; Yeo, S.; Horibe, Y.; Choi, Y. J.; Guha, S.; Croft, M.; Cheong, S.-W.; Mori, S. *Appl. Phys. Lett.* **2007**, *90*, 133123.
(5) Guiton, B. S.; Davies, P. K. *Nat. Mater.* **2007**, *6*, 586.
(6) Garcia-Martin, S.; Morata-Orrantia, A.; Alario-Franco, M. A.; Rodriguez-Carvajal, J.; Amador, U. *Chem. Eur. J.* **2007**, *13*, 5607.
(7) Martinez Sarrion, M.-L.; Mestres, L.; Morales, M.; Herraiz, M. *J. Solid State Chem.* **2000**, *155*, 280.
(8) Martinez-Sarrion, M.-L.; Mestres, L.; Palacin, R.; Herraiz, M. *Eur. J. Inorg. Chem.* **2001**, 1139.
(9) Morales, M.; Mestres, L.; Dlouha, M.; Vratislav, S.; Martinez-Sarrion, M.-L. *J. Mater. Chem.* **1998**, *8*, 2691.
(10) Morata-Orrantia, A.; Garcia-Martin, S.; Moran, E.; Alario-Franco, M. A. *Chem. Mater.* **2002**, *14*, 2871.


**10.1021/ja806130u CCC: $40.75** 

of our knowledge the Nd analogs have not previously been made. Though similar nanostructures to the ones we observe may well be thermodynamically stable for the La- and Pr-based analogs, nanoscale phase separation has not been reported, possibly because heat treatments required to form such structures were not used. Our motivation for these substitutions is not only to introduce a greater chemical difference between the phase-separated regions but also to exploit the variety of electronic and magnetic properties of these cations. For example, total segregation of Cr or Mn into one phase would result in a periodic modulation between insulating and small band gap semiconducting regions.[16−19] Additionally, a well-ordered Mn-containing phase could display orbital ordering and/or complex magnetic interactions.[19] These combinations of segregated chemistries, charge carriers, and possibly also spin interactions in addition to nanometer-spaced interfaces could well lead to exotic functionalities.

The cation ordering which leads to phase separation in $(Nd_{2/3-x}Li_{3x})TiO_3$ occurs on several levels. A prerequisite for phase separation in this system is 1:1 primary ordering to give alternating perovskite A-site (001) layers, one fully occupied by $Nd^{3+}$ cations, the second containing the $Li^+$ cations and vacancies, and the residual $Nd^{3+}$ (Figure 1, bottom right).[20−23] Secondary ordering then occurs on the nanometer length scale via phase separation within the mixed A-site layers to give the periodically arranged superlattice of nanodomains described above.[5] The atomistic driving force for phase separation most likely stems from the small, under-bonded Li cations, which displace in the [100] or [010] direction away from the A-site toward the 4-fold "square-window" sites,[24−27] and whose displacement is inhibited by adjacent Nd cations in the mixed layer.[5] This hypothesis is supported by our estimated compositions for the two phases ($(Nd_{1/2}Li_{1/2})TiO_3$ and $Nd_{2/3}TiO_3$) for which the mixed A-site layer contains only Li and no Li, respectively.

For the B-site-substituted compounds described here we predict total segregation of the $B^{3+}$ substituents for two reasons. First, for Li to totally segregate into just one of the two phases ($(Nd_{1/2}Li_{1/2})TiO_3$) charge balancing would prevent any mixing of the trivalent and tetravalent B-site cations between the two nanophases. A secondary effect for the cases of Mn and Cr is that $d^n$ cations do not undergo the displacements necessary to stabilize the primary 1:1 A-site order;[28] such layered ordering has in fact only been observed in compounds containing $d^0$ B-site cations. It should therefore be energetically favorable for these $d^n$ cations to occupy sites in a $NdB^{3+}O_3$ phase in which A-site ordering cannot occur. Finally, the $Mn^{3+}$ cations in the target $NdMnO_3$ phase are well known to show a propensity for Jahn−Teller distortion. In a disordered material this is likely to produce strain in the sample, which should provide a further driving force for phase separation on the B-sites.

## Experimental Section

Solid solutions with the general formula $x[(Nd_{1/2}Li_{1/2})TiO_3]-(1-x)[NdBO_3]$ (B = Al, Cr, Mn) were synthesized for a number of compositions using standard ceramic processing methods. $Li_2CO_3$, $Nd_2O_3$, $TiO_2$, $Al_2O_3$, $Cr_2O_3$, and $MnO_2$ powders were dried at 400, 1000, 600, 1100, 800, and 600 °C, respectively, and checked for phase purity using X-ray diffraction (XRD). Powder XRD was carried out on a Rigaku GiegerFlex D/Max-B diffractometer. $MnO_2$ decomposed during drying to produce $Mn_2O_3$ starting material. Stoichiometric mixtures of the dried binary oxides were calcined at 900 °C (for 4 h) followed by 1100 °C (overnight) and then reground followed by 1250 °C (for 24−36 h with one to two intermediate grindings). XRD was used to check phase purity; samples indexed to JCPDS file 46-0464 (Supporting Information, Figure S6).

Solid solutions for $x \geq 0.85$ (B = Al, Cr) and $x \geq 0.8$ (B = Mn) formed phase-pure 1:1 ordered perovskite from XRD contingent on the cooling rate used. To form 1:1 primary order both the Al- and Cr-substituted compositions required a cooling rate of 5−10 °C/h after the final calcinations, whereas the Mn-containing composition formed an ordered structure after a 300 °C/h cool. Further annealing (72 h) of the Mn structure resulted in both changes in the nanomorphology and growth of impurity phases as the protected pellet possibly went slightly off-composition due to lithia loss or Mn oxidation. Energy-dispersive X-ray spectroscopy (EDS) and electron energy loss spectroscopy (EELS) in the TEM were used to confirm that individual crystals all contained the respective B-site substituent in roughly the amount targeted (Supporting Information, Figure S1).

TEM images were obtained using a JEOL 2010 FEG TEM/STEM operating at 197 kV. Samples were prepared by grinding the as-synthesized powders, suspending in a chloroform solution using sonication, and dispersing on a lacey carbon/copper TEM grid. TEM images and selected area electron diffraction (SAED) patterns were taken on film, the developed negatives scanned, and image files processed using Photoshop software. Z-contrast images were recorded in STEM dark field mode with a high-angle aperture (inner radius 54.9 mrad) and processed using Digital Micrograph software.

## Results and Discussion

Figure 2 shows representative TEM images of the B-site-substituted materials. By comparison with the unsubstituted titanate (Figure 2a,b), it is apparent that the effect of substitution on the observed nanostructure and periodicity is dramatic. $0.85[(Nd_{1/2}Li_{1/2})TiO_3]-0.15[NdAlO_3]$ shows a striking stripe and chessboard combination (Figure 2c,d). The stripes can effectively be described as the resulting morphology from stacking faults parallel to (010) in the chessboard. Corresponding SAED patterns show a wealth of sharp satellite peaks with periodicities in the $x$ direction of $18a_p$ (∼6.9nm) and in the $y$ direction of $20a_p$ (∼7.7nm), evidence that the extremely periodic nature of the chessboard foundation has not been lost on substitution.

(11) Moreno, I.; Morales, M.; Martinez Sarrion, M. L. *J. Solid State Chem.* **1998**, *140*, 377.
(12) Ruiz, A. I.; Lopez, M. L.; Pico, C.; Santrich-Badal, A.; Veiga, M. L. *J. Solid State Chem.* **2003**, *173*, 130.
(13) Yang, K.-Y.; Fung, K.-Z. *J. Power Sources* **2006**, *159*, 301.
(14) Yang, K.-Y.; Fung, K.-Z.; Leu, I.-C. *J. Alloys Compd.* **2007**, *438*, 207.
(15) Morales, M.; Martinez Sarrion, M. L. *J. Mater. Chem.* **1998**, *8*, 1583.
(16) Tripathi, A. K. *J. Am. Ceram. Soc.* **1980**, *63*, 475.
(17) Taguchi, H.; Nagao, M.; Takeda, Y. *J. Solid State Chem.* **1995**, *114*, 236.
(18) Martin-Carron, L.; Ramirez, R.; Prieto, C.; de Andres, A.; Sanchez-Benitez, J.; Garcia-Hernandez, M.; Martinez, J. L. *J. Alloys Compd.* **2001**, *323−324*, 527.
(19) Zhou, J.-S.; Goodenough, J. B. *Phys. Rev. B* **2003**, *68*, 144406.
(20) Rooksby, H. P.; White, E. A. D.; Langston, S. A. *J. Am. Ceram. Soc.* **1965**, *48* (9), 447.
(21) Iyer, P. N.; Smith, A. J. *Acta Crystallogr.* **1967**, *23*, 740.
(22) Abe, M.; Uchino, K. *Mater. Res. Bull.* **1974**, *9*, 147.
(23) Lee, H. J.; Park, H. M.; Oh, S. H.; Cho, Y. K.; Son, J. O.; Nahm, S. *Jpn. J. Appl. Phys.* **2004**, *43* (11A), 7592.
(24) Alonso, J. A.; Sanz, J.; Santamaria, J.; Leon, C.; Varez, A.; Fernandez-Diaz, M. T. *Angew. Chem., Int. Ed.* **2000**, *39* (3), 619.
(25) Sanz, J.; Alonso, J. A.; Varez, A.; Fernandez-Diaz, M. T. *J. Chem. Soc., Dalton Trans.* **2002**, *7*, 1406.
(26) Sommariva, M.; Catti, M. *Chem. Mater.* **2006**, *18* (9), 2411.
(27) Catti, M. *Chem. Mater.* **2007**, *19*, 3963.
(28) Knapp, M. C.; Woodward, P. M. *J. Solid State Chem.* **2006**, *179*, 1076.

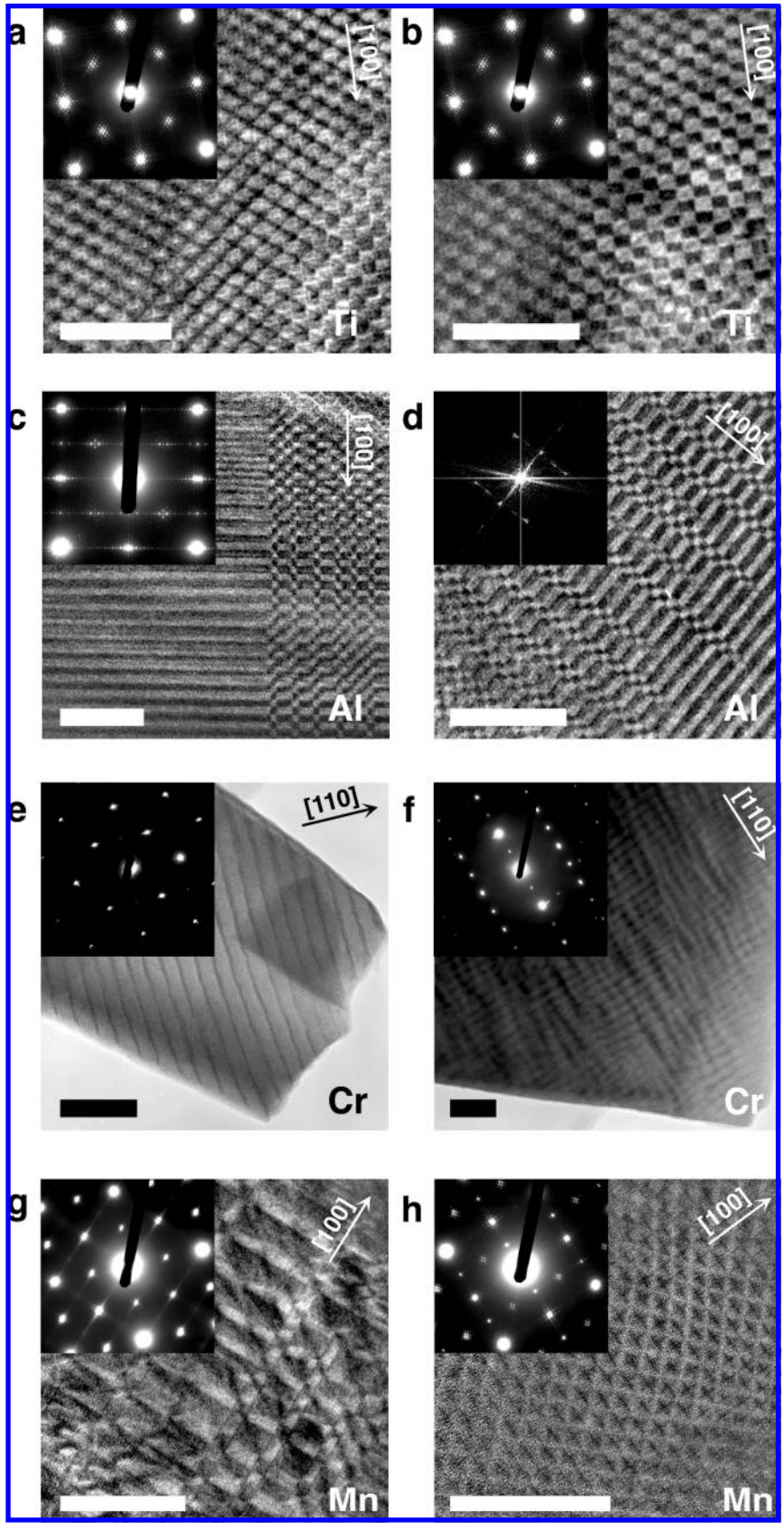


***Figure 2.*** TEM images of nanostructure morphologies. (a−h) TEM images displaying nanostructures formed by substitution of $Ti^{4+}$ by trivalent cations, with selected area electron diffraction patterns inset. Nominal compositions are $0.85[(Nd_{1/2}Li_{1/2})TiO_3]-0.15[Nd_{2/3}TiO_3]$ (a and b), $0.85[(Nd_{1/2}Li_{1/2})TiO_3]-0.15[NdAlO_3]$ (c and d), $0.85[(Nd_{1/2}Li_{1/2})TiO_3]-0.15[NdCrO_3]$ (e and f), and $0.8[(Nd_{1/2}Li_{1/2})TiO_3]-0.2[NdMnO_3]$ (g and h). Images were taken in the [001] zone (a−d, g, and h), $[1\bar{1}2]$ zone (e), $[1\bar{1}4]$ and zone (f). The material in g was annealed for 72 h to produce the sample shown in h. In the absence of SAED the inset to d is a power spectrum of the image, representative of the central beam and its satellite reflections only. Scale bars are 50 nm.

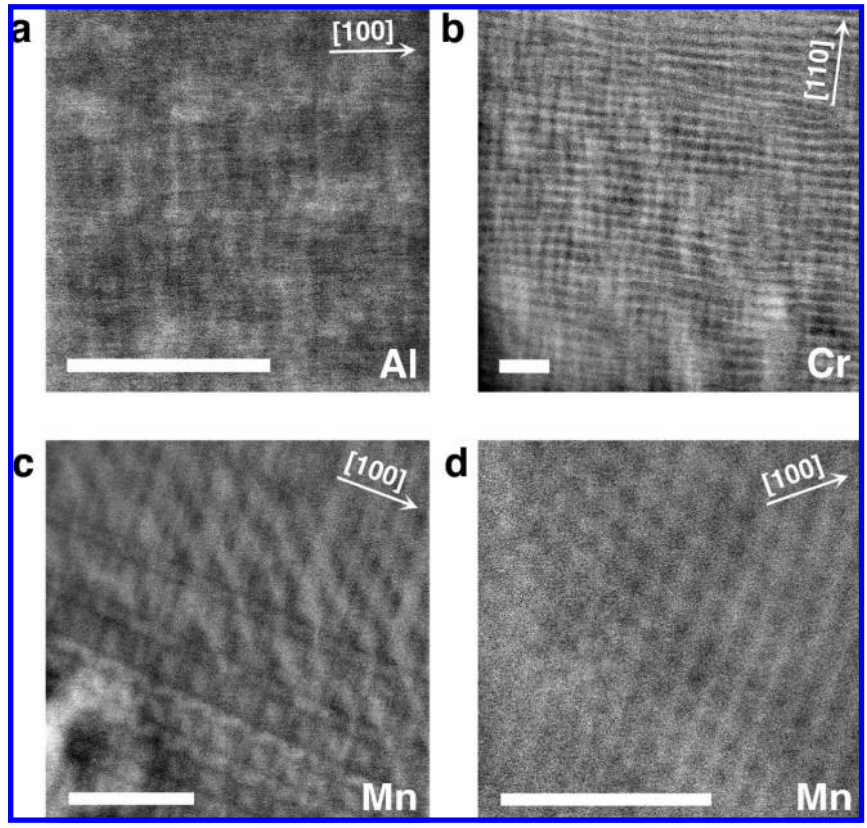


***Figure 3.*** Z-contrast images showing nanometer-scale phase separation in compounds with nominal composition $0.85[(Nd_{1/2}Li_{1/2})TiO_3]-0.15[NdAlO_3]$ (a), $0.85[(Nd_{1/2}Li_{1/2})TiO_3]-0.15[NdCrO_3]$ (b), and $0.8[(Nd_{1/2}Li_{1/2})TiO_3]-0.2[NdMnO_3]$ (c and d). The material in c was annealed for 72 h to produce the sample shown in d. Morphologies correspond to TEM images shown in Figure 2d (a), 2f (b), 2g (c), and 2h (d), respectively. Scale bars are 50nm.

The Cr-based sample $0.85[(Nd_{1/2}Li_{1/2})TiO_3]-0.15[NdCrO_3]$ exhibits a lamellae structure in which the lamellae appear to run in either one or two dimensions depending on the crystal zone (Figure 2e,f). Seen consistently across all the observed crystallographic zones are lamellae parallel to the (110) plane with an average spacing of ~10−12nm. This suggests a [110]/[$\bar{1}$10] soft direction in common with the nanochessboard morphologies. The nanostructure does not display long-range periodicity, as evidenced by diffuse streaks but no sharp satellites in the corresponding SAED pattern. The patterns seen for this material are in fact far more reminiscent of those typically found for spinodally decomposed structures. A second modulation of roughly twice the period and with a much greater dispersion of periodicities is evident parallel to ($\bar{2}$21) when imaged in the [1$\bar{1}$4] zone.

The Mn-based sample $0.8[(Nd_{1/2}Li_{1/2})TiO_3]-0.2[NdMnO_3]$ showed perhaps the most complex response, which depended on heat treatment of the material. For the sample calcined for 24 h a pseudochessboard structure is seen which does not display long-range periodicity but is systematically constructed from a set of 4−5 discrete building blocks ranging from as small as ~8 nm to as large as ~75 nm (Figure 2g). Annealing the material for a further 72 h results in an extremely periodic nanometer-scale diamond-type structure (Figure 2h) with arresting similarity to the original titanate (Figure 2a). Periodicities measured from the SAED pattern are $22a_p$ (~8.4 nm) in the $x$ direction and $28a_p$ (~10.7 nm) in the $y$ direction. Compositional analysis shows that Mn is indeed present in both the pseudo- and regular chessboard at roughly the 20% proportion of B-sites expected (Supporting Information, Figure S1). Additional unindexed peaks are seen in the XRD pattern of the annealed sample (Supporting Information, Figure S6e), which could be due to neodymium titanate and manganite impurity phases, a small degree of lithia loss, or structural changes resulting from a small amount of $Mn^{3+}$ to $Mn^{4+}$ conversion. Considering that the structures form in both cases without the need to slow cool the sample, it is likely that a very small number of vacancies are present due to changes in the Mn oxidation state.

To probe the compositional modulations in the samples Z-contrast imaging was employed (Figure 3). Clear compositional modulations are seen, as evidenced by modulations in intensity where brighter regions signify higher atomic mass, Z, for both the $NdCrO_3$- and $NdMnO_3$-substituted compounds, confirming that the nanostructures imaged arise from periodic phase separation. Modulations for the Al-substituted compound are also visible but less well defined, which is consistent with a smaller difference in Z between $(Nd_{1/2}Li_{1/2})TiO_3$ and $NdAlO_3$ than with the Mn- and Cr-substituted counterparts (19.5, 30.5, and 31.5 per formula unit, respectively). The modulations in Z-contrast are consistent with the morphologies seen in the TEM images and the corresponding predicted patterns of phase separation. In particular, the pseudochessboard pattern appears to arise from regions of the Mn-rich phase lying diagonally across the rectangular blocks, which develop into a zigzagging arrangement in the more regular chessboard regions. The periodic chessboard in the annealed sample arises from the familiar zigzagging diamond-like pattern, as is seen for the original titanate chessboard. In all cases the bright modulations correspond to the minority "boundary region" phase in the TEM images, which is consistent with this being the heavier $NdBO_3$ phase. In addition, faint modulations in the Ti energy-filtered

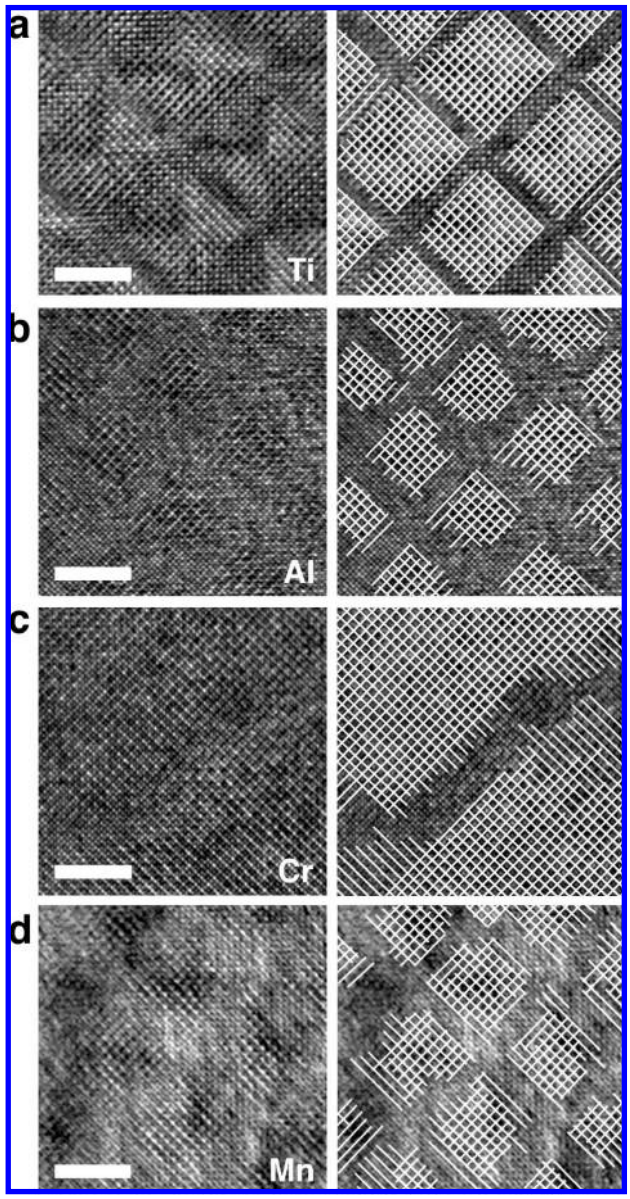


***Figure 4.*** Atomic structure. (Left) TEM images showing the atomic structure of each compound taken in the [001] zone. Nominal compositions are $0.85[(Nd_{1/2}Li_{1/2})TiO_3]-0.15[Nd_{2/3}TiO_3]$ (a), $0.85[(Nd_{1/2}Li_{1/2})TiO_3]-0.15[NdAlO_3]$ (b), $0.85[(Nd_{1/2}Li_{1/2})TiO_3]-0.15[NdCrO_3]$ (c), and $0.8[(Nd_{1/2}Li_{1/2})TiO_3]-0.2[NdMnO_3]$ (d). Scale bars are 5 nm. (Right) The same images with sketches of $(1/2\ 1/2\ 0)_p$ planes superimposed. Doubling of the (110) plane *d* spacing and an antiphase boundary between adjacent domains (features previously identified as representative of the $(Nd_{1/2}Li_{1/2})TiO_3$ atomic structure) are seen in all four cases.

TEM (EFTEM) images have also been observed, which could only occur with B-site phase separation (Supporting Information, Figure S2).

Further confirmation of phase separation is seen in the atomic structure imaged at high resolution by TEM. A distinctive feature of the $(Nd_{1/2}Li_{1/2})TiO_3$ nanodomain regions of the original chessboard was a doubling of the (110) plane spacing and an antiphase relationship of this lattice spacing between adjacent nanodomains (Figure 4a). This feature was previously suggested to result from a cooperative displacement of the Li and Ti cations, consistent with multislice TEM image simulations. This feature is seen in the majority phase of all three B-site-substituted compounds (Figure 4), consistent with Li segregated into $(Nd_{1/2}Li_{1/2})TiO_3$ regions, separated by $NdB^{3+}O_3$ boundary regions accommodating Al, Cr, or Mn on the B-site. Sketches of the regions showing the distinctive (110) doubling are given in the right-hand side panels of Figure 4. This can be used to give rough estimates of the nanoscale morphologies and ratios of the two phases, although caution must be taken, it is not facile to estimate the position of the compositional interface, not only because it does not appear to be atomically flat but also because the magnitude of Li and Ti displacements will likely decrease toward the interface, leaving it difficult to observe (110) doubling in this region. It is also likely that lithia loss due to beam damage will affect the integrity of the images. All of these reasons notwithstanding, it is clear that the majority phase in all four cases resembles the $(Nd_{1/2}Li_{1/2})TiO_3$ phase, which implies that the $B^{3+}$ substituents are segregated into the minority boundary region. For the diamond-type features seen for both Mn and especially Al, however, the boundary region is somewhat larger than that of the unsubstituted Ti B-site compound, so it is possible that the minority phase may contain small amounts of Li and Ti. Considering the low- and high-resolution TEM images and compositional data the evidence in its entirety suggests that the majority phase has a composition at or close to $(Nd_{1/2}Li_{1/2})TiO_3$ and the minority phase is $(Nd_{1-x/2}Li_{x/2})(B^{3+}{}_{1-x}Ti_x)O_3$ (where $x \ll 1$) which means, equivalently, that nanometer-scale phase separation has occurred on both the A and the B sites of these perovskite materials.

The three B-site-substituted compounds reported here have striking differences, especially with respect to their nanoscale morphologies. In changing the nominal composition of the boundary region to $NdAlO_3$, $NdCrO_3$, or $NdMnO_3$, we are introducing not only new electronic and magnetic features to the solid solution but also structural differences, such as anisotropy of the *a* and *b* parameters,[17] Jahn−Teller distortions,[18,19,29] orbital order−disorder transitions,[19] and corresponding differences in interfacial energy, which clearly greatly influence the ground-state morphology.[30] In addition, by removing vacancies from the system we reduced the kinetics of formation and may possibly be isolating intermediate morphologies part way between the disordered crystal and the final low-energy chessboard. Indeed, this is supported by the observation that further annealing the Mn-substituted sample leads to a conversion from nonperiodic pseudochessboard to periodic chessboard. An example of a stripe to chessboard conversion via a shear transformation is illustrated in Supporting Information, Figure S3.

## Conclusion

We successfully synthesized three new compounds related to the $(Nd_{2/3-x}Li_{3x})TiO_3$ nanochessboard structures through partial substitution of Ti on the B-site by trivalent cations. By a combination of imaging and compositional analysis techniques we demonstrated that these compounds periodically phase separate on both the A- and the B-sites of the perovskite structure. The extremely periodic nature of the chessboard can be maintained using specific compositions and/or heat treatments. The generality of composition that demonstrates this spontaneous compositional nanopatterning is extremely promising for a wide array of exotic bulk and nanostructural properties.

**Acknowledgment.** We thank D. M. Yates for technical support. This work was supported by the National Science Foundation, under grant DMR0704255, and by the MRSEC Program, under award no. DMR05-20020.

(29) Kamegashira, N.; Miyazaki, Y. *Phys. Status Solidi A* **1983**, *76*, K39.
(30) Ni, Y.; Jin, Y. M.; Khachaturyan, A. G. *Acta Mater.* **2007**, *55*, 4903.

**Note Added in Proof.** Garcia-Martin et al.[31] recently reported compositionally modulated stripe phases in the $NaLaMgWO_6$ perovskite system. This exciting result suggests that spontaneous nanometer-scale phase separation could be a more general phenomenon and more widespread than previously appreciated.

(31) Garcia-Martin, S.; Urones-Garrote, E.; Knapp, M. C.; King, G.; Woodward, P. M. *J. Am. Chem.* **2008**, *130*, 15028.

**Supporting Information Available:** Compositional analysis data (EDS and EELS), EFTEM images, an illustration of a possible mechanism for phase separation, and XRD data and simulations can be found in the Supporting Information. This material is available free of charge via the Internet at http://pubs.acs.org.

JA806130U